Brittle Fracture of an Au/Ag Alloy Induced by a Surface Film

R.G. KELLY, A.J. FROST, T. SHAHRABI, and R.C. NEWMAN

The film-induced cleavage model of stress-corrosion cracking (SCC) has been tested using an Ag-20 at. pct Au alloy in 1 M $HClO_4$ solution. Brittle cracks, both intergranular (IG) and transgranular (TG) in nature, were formed by high-speed loading of a thin foil covered with a dealloyed (nanoporous gold) layer. These cracks were found to propagate through the dealloyed layer and into the uncorroded bulk face-centered cubic (fcc) material for a distance of many microns. Hydrogen embrittlement (HE) can be excluded on thermodynamic grounds; thus, only film-induced cleavage can explain the observed decoupling of stress and corrosion in the fracture process.

I. INTRODUCTION

THE long history of the study of stress-corrosion cracking (SCC) of metals and alloys has resulted in many proposed models, including slip dissolution,[1,2,3] hydrogen embrittlement (HE),[4,5,6] adsorption-induced brittle or plastic fracture,[7,8,9] and film-induced cleavage.[10,11,12] Some models, including the adsorption models[7,9] and the more recent surface mobility model[13] propose that all forms of environmentally assisted fracture [SCC, HE, liquid metal embrittlement (LME)] occur by the same mechanism. Other models are proposed to be less widely applicable. In the following sections, the different SCC and HE models are briefly reviewed, and their predictions are examined closely.

A. *Slip Dissolution*

In slip dissolution models, cracking is ascribed to the localized dissolution of the alloy, with the stress acting to supply localized plastic strain which ruptures a protective film. Thus, the maximum crack velocity can be related *via* Faraday's Second Law to a crack tip current density:

$$i_{ct} = \frac{vn\rho F}{M\beta}$$

where i_{ct} = crack tip dissolution rate;
v = crack velocity;
n = number of electrons transferred;
ρ = density of dissolving material;
F = Faraday's constant;
M = mean atomic weight; and
β = atom fraction of dissolving material.

While some cases of intergranular SCC (IG-SCC) can be explained in this way, as done by Ford[14] and Parkins,[15] Galvele[13] has recently pointed out that there is a limit to the crack velocity that can be reasonably expected due solely to dissolution. However, this limit may be higher than suggested by Galvele: recent work by Rota and Böhni[16] on Al-Cu suggests that dissolution can readily supply current densities of 0.5 A/cm^2, equivalent to 0.2 μm/s for Fe $\rightarrow$ Fe^{2+}, and typical for the classic IG-SCC system of mild steel in nitrate solution,[15] among others. Where the IG crack velocity is extremely high, *e.g.*, 10 μm/s in Au-Cu or Au-Ag[17,18] or sensitized stainless steel in thiosulphate,[19] the required crack tip current density of many A/cm^2 would be impossible to achieve on ohmic and diffusional grounds. In addition, the interlocking fracture surfaces, cleavage-like morphology, and crack arrest markings found in transgranular SCC (TG-SCC) are difficult to explain based upon a dissolution model.[20]

B. *Surface Mobility*

Recently, Galvele[13] has analyzed all types of environmentally assisted fracture in terms of a continual egress of atoms from the crack tip by surface diffusion. He explains cracking in terms of a stress-induced increased surface mobility of a low melting point surface compound formed from the base material and a component of the environment and shows good correlations between measured and predicted crack velocities for a number of systems.[13] These correlations are based upon fitting a surface diffusivity to the actual crack velocity data *via* an equation derived on the basis of the thermal equilibrium concentration of vacancies. With no independent method of measurement of the surface diffusivity or the presence of the proposed aggressive surface compounds, verification of the model in any particular system is difficult. This model is very similar to that proposed by Tiller,[21] but Galvele has provided a detailed rationalization of experimental data.

C. *Hydrogen Embrittlement*

Hydrogen embrittlement models abound.[4–8] Most models involve the generation of atomic hydrogen at the crack tip with its subsequent absorption into the material and bulk diffusion to certain microstructural sites.[5,6] The accumulation of hydrogen at these sites leads to a reduction in the work to fracture. Other models postulate a near-surface hydrogen effect. The hydrogen adsorption theory of Petch and Stables[8] postulates that the reduction in the surface free energy of a crack by the adsorption of hydrogen is sufficient to lower the fracture stress

R.G. KELLY, Research Assistant Professor, is with the Department of Materials Science and Engineering, University of Virginia, Charlottesville, VA 22903. A.J. FROST, Technical Investigator, is with the Steel Products Group, British Steel Technical, Swinden Laboratories, Moorgate, Rottenham, S. Yorks, England. T. SHAHRABI, Assistant Professor, is with the Materials Department, Tarbiat Modarres University, Tehran, Iran. R.C. NEWMAN, Senior Lecturer, is with the Corrosion and Protection Center, University of Manchester, Institute of Science and Technology, Manchester M60 1QD, United Kingdom.

Manuscript submitted January 3, 1990.

necessary based upon the Griffith criterion to the point that cracking occurs. Oriani[4] has proposed a slightly different model, wherein the hydrogen reduces the cohesive force between the atoms near the crack tip, leading to a decrease in the stress necessary for fracture. Lynch[7] proposes that the adsorbed hydrogen acts to allow localized easy slip to occur at the crack tip, with this process leading to the appearance of cleavage-like fractography. Generally, it is quite difficult to categorically exclude hydrogen as the cause for cracking, especially in cases where changes in crack tip chemistry can occur which favor hydrogen production at the crack tip.[22] However, there are cases, notably gold alloys, where it can be excluded on thermodynamic grounds.[23]

D. *Adsorption-Induced Brittle or Ductile Fracture*

Uhlig[9] extended the adsorption-based theory of Petch and Stables[8] from hydrogen-induced cracking to SCC. This model explains brittle failure by the reduction of the metal-to-metal bond strength at the crack tip *via* adsorption of aggressive species. Instead of this bond-by-bond brittle fracture, Lynch[7] has proposed that SCC, as well as HE and LME, is due to the continuous adsorption of an aggressive species at the crack tip, which weakens the bonding but results in highly localized easy slip, similar to the hydrogen-induced plasticity model of Beachem.[24] Both models are intended to be universally applicable to all forms of environmentally assisted cracking. Since adsorption at room temperature is a relatively fast process, such models could account for the high crack velocities sometimes observed in SCC and LME, though they are also applicable to cases of slow cracking.

E. *Film-Induced Cleavage*

Sieradzki and Newman[10,11] recently proposed a film-induced cleavage model derived in part from the early work of Edeleanu and Forty.[12] This model is based upon the idea that a crack, originating in a surface layer, can obtain a high enough velocity to propagate for some distance into the unattacked substrate even if the latter is face-centered cubic (fcc). In this model, like some variants of the HE model, the effects of stress and corrosion are decoupled. The role of the environment is to produce a surface film with nanometer-scale porosity (often a dealloyed layer, as shown in the case of α-brass in ammonia,[25]) while the role of the stress is to initiate a crack in the film with a sufficient velocity to propagate into the base material as a limited cleavage fracture. This combination of corrosion and mechanical processes is then repeated at the tip of the newly formed cleavage crack. In referring to this process as cleavage, it is recognized that significant dislocation activity will occur—indeed, the arrest of the crack has been analyzed quantitatively as due to exhaustion by periodic dislocation emission.[10,11] The average crack tip radius is probably at least twice the close-packed interatomic distance.

F. *Predictions of Each Model*

A comparison of the predictions of the various SCC models is useful in devising experiments to test the applicability of each to a given stress-corrosion system. Five aspects of SCC phenomena will provide the framework for comparing the four types of models: (a) the continuity of the cracking, (b) the response to impact loading, (c) the necessity for hydrogen ion or water reduction, (d) the necessity for the continual presence of the aggressive environment (*i.e.*, can stress and corrosion be decoupled ?), and (e) the reversibility of the embrittlement.

1. *Continuity of cracking*

The question as to whether cracks propagate in a continuous manner or in a series of bursts has been discussed for many years. It is widely accepted that there are examples of both types of stress-corrosion systems in practice.[20] In this paper, we are only concerned with the predictions of each model with respect to the continuity of cracking. The slip dissolution model, the surface mobility model, and the adsorption-induced plasticity model predict cracking to occur in an essentially continuous manner, while some HE models and the film-induced cleavage model predict discontinuous crack advance. The periods between crack advance events are necessary in the latter two models to allow time for the hydrogen to absorb and diffuse to the critical sites and for the nanoporous layer to form, respectively.

2. *Response to impact loading*

While most stress-corrosion testing is done under slow strain rate conditions, the predictions of each type of model with respect to the response to impact loading can be used to determine their applicability in a given system. Due to the intimate interaction between the stress and the corrosion in the slip dissolution model, a marked effect of strain rate is predicted. Slip dissolution (and, similarly, the surface mobility model) is inoperable under conditions of high strain rate due to the lack of time necessary for dissolution to occur. In other words, the slip dissolution model would predict that a susceptible material would not crack if it were first exposed unstressed to the aggressive environment for any given period of time and then strained rapidly to failure. In fact, this is the motivation for the slow strain rates utilized in slow strain rate testing.[26] For similar reasons, adsorption-induced plasticity models would also predict no cracking to occur under impact loading conditions, though due to the speed of adsorption, somewhat higher crack velocities can be explained, and therefore higher strain rates can be tolerated as compared to the slip dissolution model. Some HE models, on the other hand, due to the decoupling of the effects of stress and the aggressive environment, are operable under impact loading. If a sample were charged with hydrogen and then impact loaded, these models would predict that a crack would propagate through some of the region of the sample into which the hydrogen had diffused. As discussed above, film-induced cleavage model also decouples the effects of stress and the aggressive environment and, hence, can also operate under impact loading conditions. According to this type of model, once the critical dealloyed (or similar) layer is formed, the stress acts to initiate the crack in the layer at a sufficient velocity to penetrate the substrate. Due to the inherent macroscopic brittleness of these nanoporous layers,[27] the loading rate is of little importance to the crack initiation and propagation.

3. *Necessity of hydrogen evolution*

Obviously, only the HE models require hydrogen evolution to occur. While the other models require some cathodic reaction to occur under free-corrosion conditions, that reaction does not need to produce hydrogen, nor does it need to occur at the crack tip.

4. *Necessity of the presence of the aggressive environment*

Neither the film-induced cleavage model nor the HE model fundamentally require the simultaneous presence of a liquid environment and a tensile stress. In fact, once the dealloyed layer is formed (or the hydrogen is absorbed and diffuses to the appropriate sites), the liquid environment is superfluous, and the material could be strained outside of the environment and still fracture in a brittle manner (at least to a limited extent). Both the slip dissolution model and the absorption-induced plasticity models require the continual presence of a liquid environment to support the electrochemical reactions and to allow adsorption of the aggressive species to occur, respectively. In the surface mobility model, limited cracking out of the environment can theoretically occur, utilizing material adsorbed on the crack tip and walls. However, this would occur at the same (slow) rate as in the normal cracking environment.

5. *Reversibility of the embrittlement*

Finally, only the HE model and the film-induced cleavage model predict an aging effect in the ability to form a crack in the absence of the aggressive environment. In the case of HE, given sufficient time and temperature, the hydrogen that has been charged into the material will disperse or diffuse out, reversing the embrittlement. For the film-induced cleavage model, the nanoporosity of the dealloyed layer is highly unstable and can coarsen significantly by surface diffusion at room temperature.[25,28] Therefore, like the HE model, an aging effect is expected. For the slip dissolution model, since the cracking is continuous, no aging effects would be predicted.

G. *SCC of Noble Metal Alloys*

On the basis of these different predictions of the various SCC models, one can look for a combination of alloy and environment that would allow a fairly unambiguous determination of the cracking mechanism. The SCC of noble metal alloys is such a system.

The SCC of noble metal alloys is well-documented[17,18,29–36] and has been carefully correlated with dealloying in noble metal alloys by Graf and Budke.[17,18] Further work showing the importance of dealloying was done by Bakish and Robertson,[30] as well as by Pickering and Swann.[38] Hydrogen embrittlement of Au-Cu or Au-Ag can be categorically ruled out under anodic polarization based upon the thermodynamic calculations of Bertocci.[23] Thus, the possible models for the observed cracking are slip dissolution (dealloying with periodic rupture of the layer but no brittle fracture of the substrate), adsorption-induced plasticity, and film-induced cleavage. The normal mode of failure in polycrystalline Au alloys, *e.g.*, Cu-25 at. pct Au in $FeCl_3$ solution,[30] is a fast IG fracture (several μm/s), but cleavage-like SCC occurs readily in monocrystals.[31] The latter has been studied recently by Cassagne *et. al.*,[32,33,34] who propose a film-induced cleavage interpretation. In view of the high crack velocities, a mechanical component of IG crack growth is also likely, but this has not been demonstrated to our knowledge. On the contrary, Duffo and Galvele[35] have proposed that IG-SCC of Au-Ag alloys occurs by a continuous process of atom egress by surface diffusion away from the crack tip, according to the surface mobility model of SCC.[13] In this model, the melting point of a surface silver compound determines the relevant surface mobility, contrary to the views of others on dealloying,[36,37] in which it is the gold that surface diffuses and permits continual dissolution of silver. This is obviously a major point of disagreement.

Successful correlation of dealloying with SCC and localized cleavage events in thin foils has been achieved for α-brass in ($Cu^+ + NH_3$) solutions;[25,39] however, Ag-Au or Cu-Au alloys are even more suitable in view of the precise electrochemical measurement and control of the dealloying process, the ability to produce dealloyed layers of different thicknesses, the lack of interfering reactions, and the chemical stability of the dealloyed layers in air.

The aim of the present work was to test the ability of dealloyed layers on an Ag-Au alloy to nucleate brittle, mechanical fracture in the unattacked substrate, using thin foils as employed by Newman *et al.* in a study of the α-brass/ammonia system.[25] By varying the testing conditions judiciously, the applicability of the various SCC models can be determined.

II. EXPERIMENTAL

The material used for this investigation was an Ag-20 at. pct Au alloy supplied by Johnson-Matthey plc (Herffordshire, United Kingdom) The ingot was then rolled by Goodfellow Metals (Cambridge, United Kingdom), into foils with nominal thicknesses of 50 and 100 μm. As shown in Figure 1, tensile samples were made by cutting rounded notches on each side of the sample. Each tensile sample was polished lightly on one side with 4000 grit abrasive paper, rinsed in deionized water, acetone, and finally methanol before annealing for 1 hour at 900 °C in air, followed by air cooling. The grains were essentially equiaxed and approximately 30 μm in diameter. The sample was then rinsed again in methanol, and all but 0.04 cm^2 of the previously polished side of the gage length was insulated with lacquer. The specimen was then inserted into a miniature tensile testing rig whose pull arm was attached to a computer-controlled solenoid, as shown schematically in Figure 2. The solenoid pulled the sample through 6 mm in approximately 75 ms. Based upon a 3-mm gage length and an elongation of 1 mm for ductile samples, this corresponds to a strain rate of 25 ± 5 s^{-1}, with even higher strain rates for the embrittled samples. This type of device allows a test of the decoupling of the stress and corrosion which, as pointed out above, provides a critical test for the applicability of the dissolution- and adsorption-based models.

The test solution was 1 M $HClO_4$ at room temperature and open to air. The test cell consisted of the miniature tensile rig with an electrical connection to the specimen

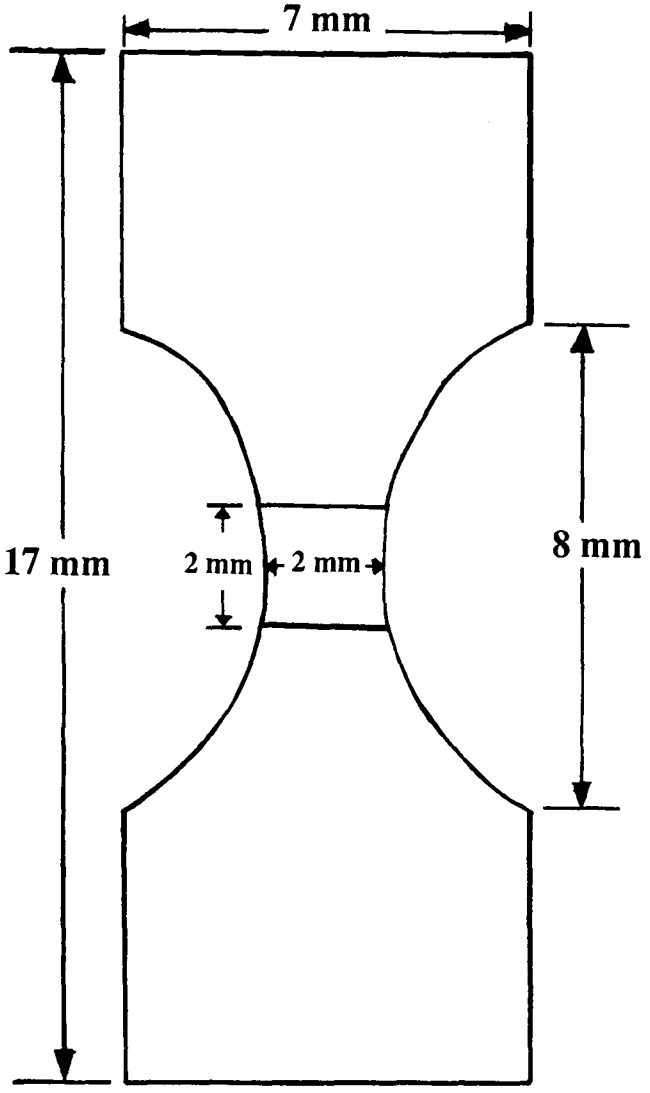

Fig. 1—Schematic of foil tensile samples used. Entire surface was masked with electroplater's lacquer except for a 2 × 2-mm area of the gage length and the electrical connection, which was made outside the solution.

and a Pt auxiliary electrode. A saturated calomel reference electrode was located in a separate compartment in order to avoid Cl^- contamination of the test solution and was connected to the solution *via* a Luggin probe. After immersion unstressed in the solution for 5 minutes at the open circuit potential (typical +0.35 V(SCE)), the potential was increased to +1.05 V(SCE), where rapid dealloying occurred. This resulted in perfectly selective removal of the Ag atoms, as the reversible potential for Au is well above this potential in this solution. After growing a dealloyed layer about 20-μm thick (2 minutes at +1.05 V and $\approx$90 mA/cm^2), various treatments were applied to the electrode before it was rapidly strained to failure ($\approx$25 s^{-1}). A 20-μm-thick layer was chosen for convenience in differentiating between cracks in the layer and those in the bulk material upon post-test examination. Some experiments using a three-point bend jig for the impact loading were also performed on the same material rolled to 0.5 mm. This facilitated metallographic mounting and viewing of the cross sections in order to evaluate any preferred path of the dealloying. Preparation of these samples was identical to that of the foils, including annealing at 900 °C for 1 hour prior to testing. While the strain rate was not measured in these tests, it is estimated to be >100 pct/s. It must be emphasized that in all cases, the samples were exposed to the solution unstressed, including the time during which the dealloyed layers were grown.

The key aspect of these experiments is the decoupling of the stress from the corrosion. As pointed out above, once hydrogen is excluded, the only model which is consistent with the formation of a crack in the absence of dissolution is the film-induced cleavage model. By introducing the stress in a "single shot" manner, other SCC mechanisms are simply not rapid enough to account for any observed cracking. This will be discussed further in later sections.

The following treatments were performed after growing the 20-μm layer:

Procedure 1: Strained rapidly to failure while maintaining the potential of the specimen at +1.05 V(SCE).

Procedure 2: Removed from the test solution, rinsed with deionized water and methanol, dried with hot air (approximately 85 °C for 2 minutes), then reimmersed in the acid and strained rapidly to failure at its open circuit potential.

Procedure 3: Removed from the test solution, plunged immediately in liquid nitrogen without rinsing, and strained rapidly to failure near 77 K.

Procedure 4: As in procedure 3, but not fractured at 77 K. Allowed to warm to room temperature before being treated as in procedure 2.

The following types of control tests were also performed:

Procedure 5: Strained rapidly to failure near 77 K without exposure to the test solution.

Procedure 6: Strained rapidly to failure at room temperature without exposure to the test solution.

All fracture surfaces were examined in a scanning electron microscope.

III. RESULTS

A typical foil fracture surface from procedure 1 is shown in Figure 3. The predominant mode of cracking is IG, though some TG cracks can also be seen which penetrate past the dealloyed layer into the bulk material for a distance of up to 40 μm. All TG cracks were observed to occur on planes which intersected the main fracture surface. None of the main fracture surface was TG in nature. The extent of the dealloyed layer is clearly visible at the top of the photomicrograph. Extensive cracking of this layer has occurred, and it is apparent that one crack propagated through an additional 80 μm of uncorroded foil. Since this cracking took place in $\leq$15 ms (based

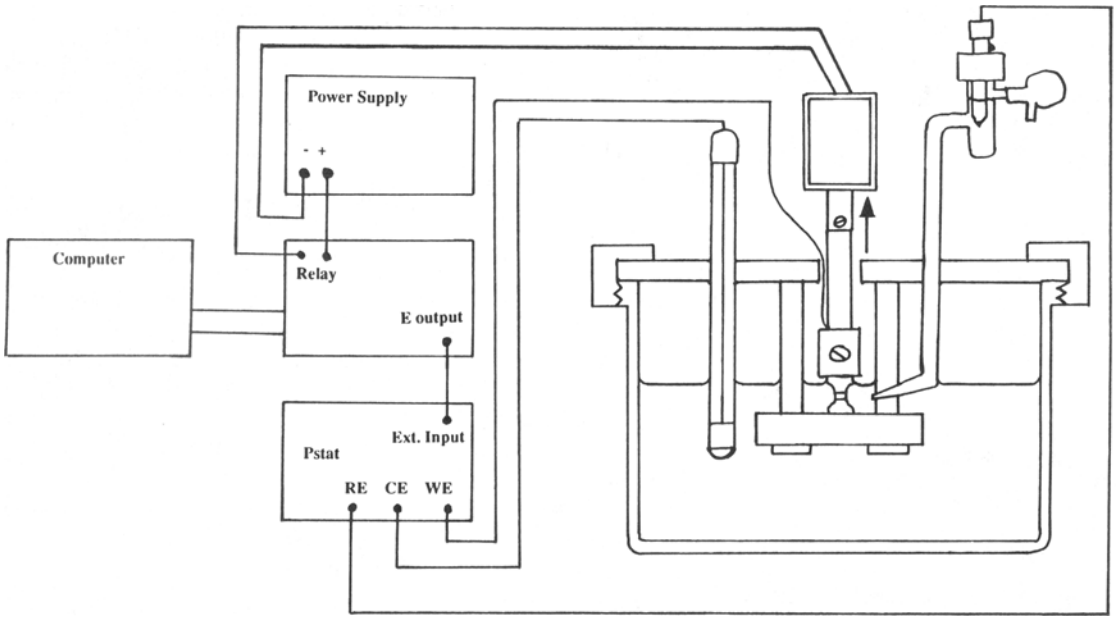

Fig. 2—Schematic of the computer-controlled testing apparatus. The action of the solenoid was triggered *via* a computer-controlled relay. The tensile testing rig itself was made of polypropylene and polytetrafluoroethylene.

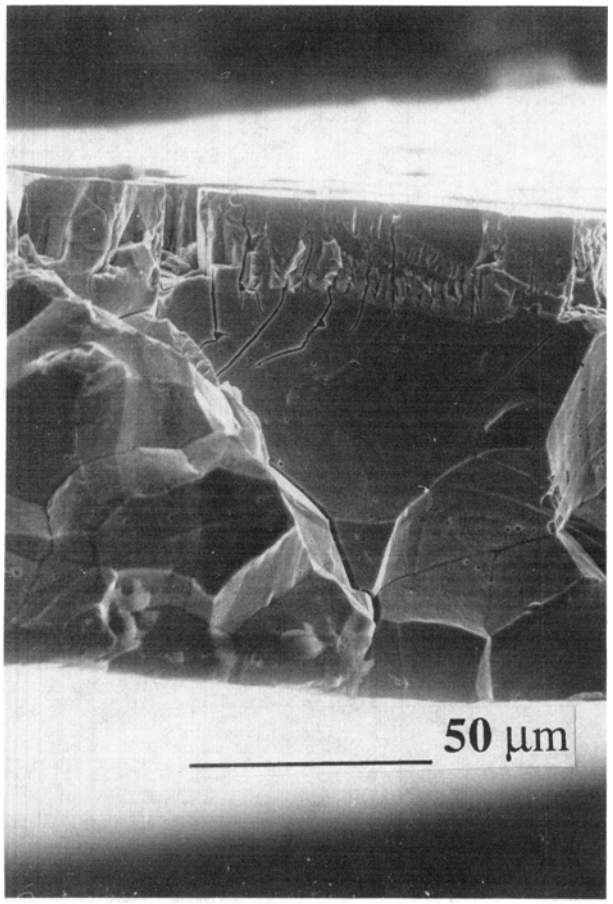

Fig. 3—Photomicrograph of fracture surface of foil sample from procedure 1 (pulled at +1.05 V). The dealloyed layer can be seen clearly at the top of the sample (20-μm thick), as can both the IG and TG cracks which propagated through it into the bulk material.

upon the strain-to-failure and the elongation rate), a crack velocity of 5 mm/s can be estimated, though the true velocity would be much higher. Figure 4 shows a cross-sectional view of a 0.5-mm sheet that was impact loaded under identical conditions in a three-point bend rig. Again, the extent of the dealloyed layer is apparent, as are the cracks which propagate well into the bulk material. The tendency for the dealloying to occur slightly preferentially at the grain boundaries is also apparent. This would be expected to lead to a concentration of the stress at these sites during the impact loading. This is supported

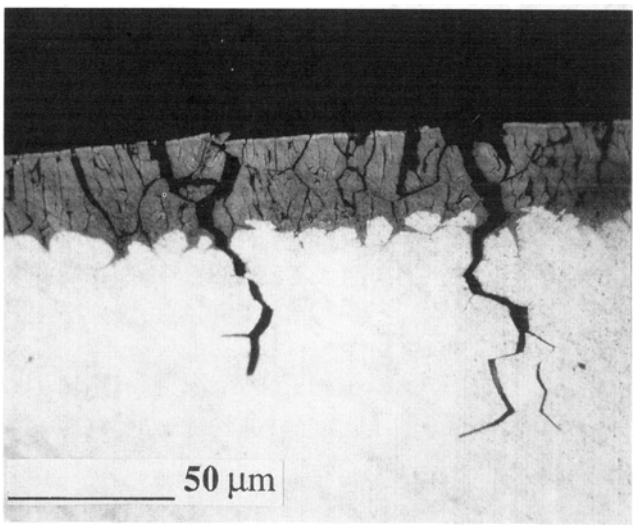

Fig. 4—Metallographic section of 0.5-mm sheet sample from procedure 1. The dealloyed layer is at the top, and cracks which propagate well past the dealloyed layer can be seen. Also, note the preferential attack of the dealloying at the grain boundaries.

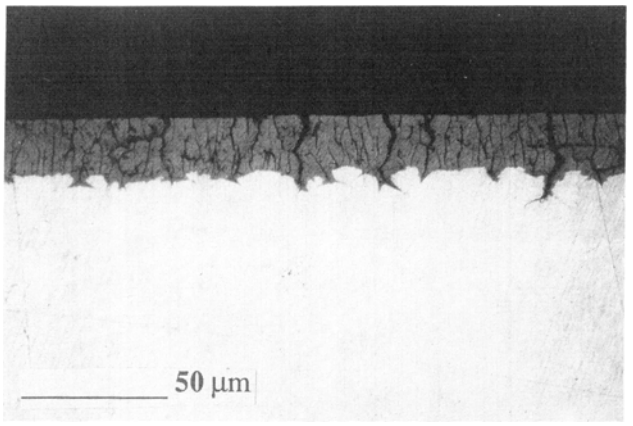

Fig. 5—Metallographic section of 0.5-mm sheet sample from procedure 2. Note the many cracks in the dealloyed layer, but none propagate into the bulk material.

by the wide openings of the cracks in the dealloyed layer at the grain boundaries (even those that do not propagate into the bulk material), which indicate that these cracks were opened at smaller strains than the other cracks in the layer.

Procedure 2 (Figures 5 and 6) shows that aging the dealloyed layer destroys its ability to nucleate brittle cracks which can propagate into the bulk material. Figure 5 shows a 0.5-mm sheet sample that was impact loaded in three-point bending after growing a dealloyed layer and allowing it to age. The layer itself remains brittle, as can be seen in Figure 5, but none of the cracks penetrate past the base of the layer. If the cracks shown in Figures 3 and 4 had been formed by SCC (due to residual stresses) during exposure at +1.05 V(SCE) before the samples were impact loaded, then they would still be observable in a sample that was removed, washed, and dried. Figure 6 shows a foil sample that was treated in the same way as the 0.5-mm sheet sample of Figure 5. As in Figure 5, the cracks are seen to stop at the interface between the dealloyed layer and the uncorroded bulk material. Identical results were obtained in tests in which the samples were not removed from the solution but simply allowed to age in the absence of any applied potential.

The fracture surface shown in Figure 7 resulted from procedure 3. This shows that these cracks can propagate even in the absence of a liquid environment, again indicating the mechanical nature of the process. It should be noted that the foil shown in Figure 7 was 50 μm in thickness, and that the main crack propagated less than

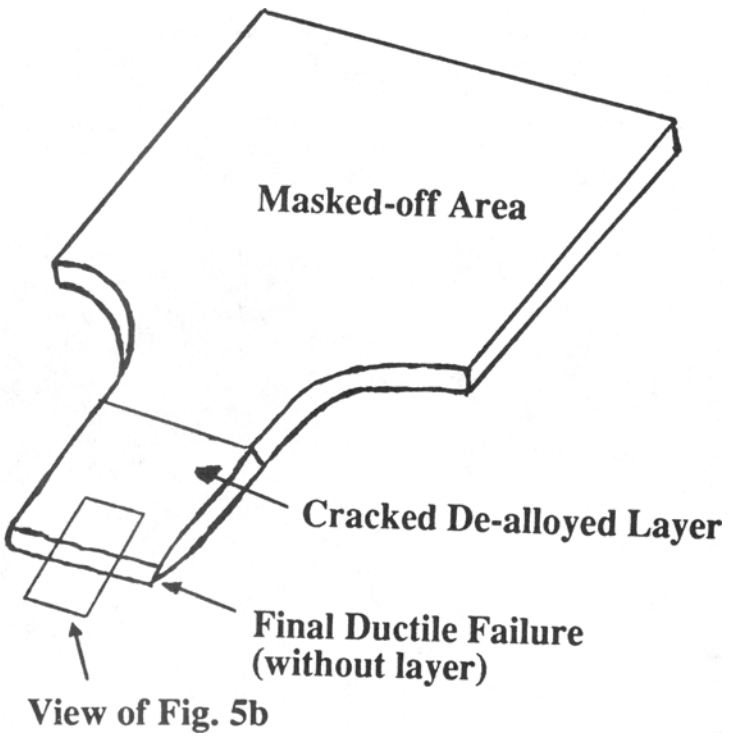

(*a*)

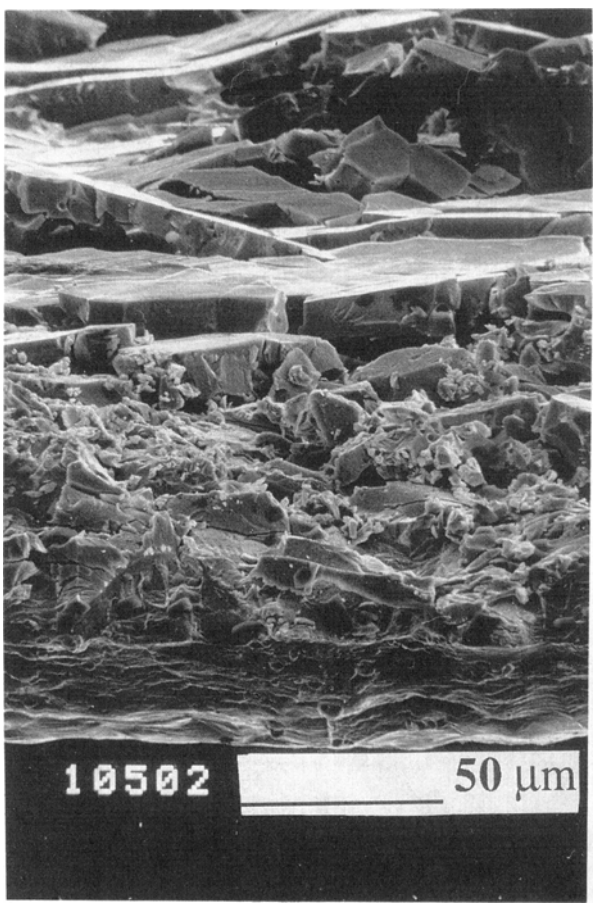

(*b*)

Fig. 6—(*a*) Schematic of appearance of foil sample from procedure 2 (pulled after aging layer). The orientation of the photomicrograph shown in (b) is indicated. (*b*) Photomicrograph of fracture surface of foil sample from procedure 2. The ductile failure of the bulk of the foil has carried the broken dealloyed layer along with it. The final fracture is free of remnants of the dealloyed layer.

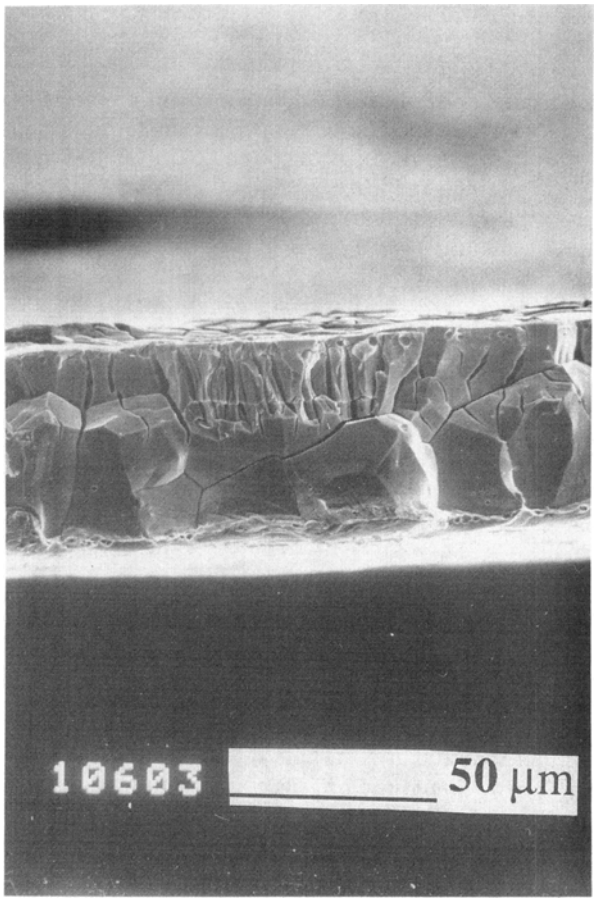

Fig. 7—Photomicrograph of fracture surface of 50-μm foil sample from procedure 3 (pulled at 77 K). Note the similarity to Fig. 4. Also note that last 5 μm of the sample (on the bottom of the micrograph) appeared to have failed in a ductile manner, indicating the limit of brittle crack advance under these conditions to be about 20 μm.

Fig. 8—Photomicrograph of fracture surface of foil sample from procedure 5 (no layer, 77 K). Note the completely ductile failure, as expected for fcc materials even at 77 K. The orientation is such that the chisel point failure of this foil is pointing straight out of the photomicrograph.

30 μm into the unattacked substrate, with the final 5 μm failing in a ductile manner. Identical results were observed for 100-μm-thick foils. However, the fractography of the 50-μm foils was much easier to photograph due to the limited amount of material which failed in a ductile manner. Face-centered cubic alloys are expected to fail in a ductile manner at 77 K, and in the absence of a dealloyed layer, the foils used in the present investigation do indeed fail in such a manner, as shown in Figure 8 (procedure 5).

The results of procedure 6, shown in Figure 9, are consistent with the normally ductile behavior of this alloy when a dealloyed layer is absent. Finally, procedure 4 also resulted in ductile failure of the bulk material, indicating that the rapid cooling of the dealloyed layer to 77 K was not the cause of the crack initiation.

IV. DISCUSSION

Unambiguous testing of the various SCC models is generally extremely difficult. Typically, more than one model is consistent with the experimental observations; HE is especially difficult to rule out categorically, owing to changes in crack tip chemistry which favor the local production of hydrogen. However, the present work presents a case of SCC in which the fundamental processes in the different proposed models can be experimentally eliminated or controlled, allowing for an unambiguous determination of the applicable model.

For the case of Cu-Au alloys in $FeCl_3$, Bertocci[23] has shown that it is thermodynamically impossible for hydrogen to be produced, even in a growing crack. This would also, obviously, be true for the case of Ag-Au alloys in perchloric acid. Based upon Bertocci's calculations, we estimate that we are operating at least 600 mV above the reversible potential for hydrogen evolution. Hence, as with Cu-Au, the possibility of HE as a cause of the SCC Ag-Au can be categorically ruled out, as the generation of hydrogen would occur at an activity of $<10^{-10}$ for a potential 600 mV above the standard reversible potential. The predictions of the remaining models (slip dissolution, surface mobility, adsorption-induced fracture, and film-induced cleavage) are shown in Table I and compared with the experimental results.

A comparison of Table I and Figures 3 through 9 shows that only the film-induced cleavage model is able to rationalize the experimental results. In the case of procedure 1, the crack tip dissolution rate necessary to account for the observed crack velocity can be calculated. By using the appropriate values for the Ag/Au alloy used in this investigation and a crack velocity of 5 mm/s (based upon cracking through 80 μm of material in 15 ms), a

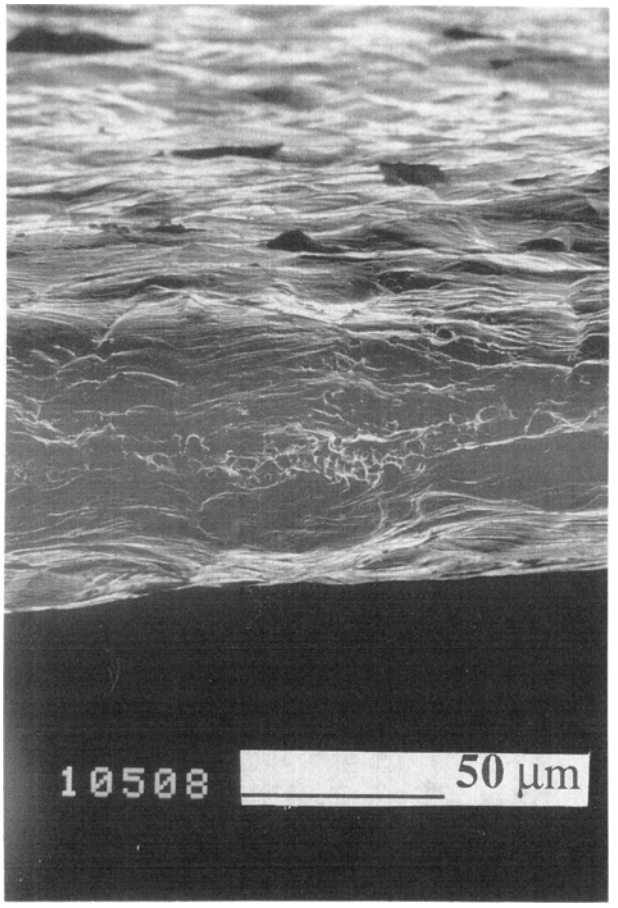

Fig. 9—Photomicrograph of fracture surface of foil sample from procedure 4 (no layer, 298 K). Note the completely ductile failure. This sample is tilted downward slightly with respect to that of Fig. 8.

crack tip dissolution rate of 5,800 A/cm^2 would be necessary to account for the observed cracking. Obviously, this is impossible. In addition, this same current density would have to be supplied at 77 K in the absence of external circuitry and a liquid environment in order to explain the results of procedure 3. The possibility that dealloying occurred along the grain boundaries during the formation of the layer and that it was this thin gold sponge that cracked during the subsequent straining can be ruled out on the basis of procedure 2. If such a dealloyed path had formed, the aging treatment would not have increased its strength to the level of the uncorroded material. On the basis of these considerations, it is obvious that the slip dissolution mechanism can be ruled out as the cause of the observed cracking in this system.

The surface mobility model of Galvele[13] is readily quantifiable, given a knowledge, or estimate, of the crack tip conditions, according to the following equation:

$$v_p = \frac{D_s \sigma \alpha^3}{LkT}$$

where v_p = crack velocity;
D_s = surface diffusivity;
σ = elastic surface stress at crack tip;
a = atom size;
L = diffusion distance of the adatoms or vacancies;
k = Boltzmann constant; and
T = temperature.

Using the estimate of a 5 mm/s crack velocity, a diffusion distance of 10^{-8} m (as used by Galvele),[13] an atom size of 2.5 Å, and a crack tip stress of 1 GPa, we can determine that a surface diffusivity on the order of 10^{-12} m^2/s is required to account for the cracking. It is worth mentioning that such a crack tip stress will be an overestimate based upon the work of Rice and Johnson,[41] in which it is estimated that the maximum stress at the tip of a crack cannot exceed four to five times the tensile yield stress of the material, even for materials which strain harden as much as low-strength steels. Therefore, the estimate of a necessary surface diffusivity of 10^{-12} cm^2/s is a conservative one, favorable to the applicability of the surface mobility model. While this appears to be a reasonable value for cracking at 298 K (procedure 1), it is not apparent what surface compound could be responsible under the present experimental conditions. Even more importantly, the results at 77 K (procedure 3) must also be explained in terms of surface diffusion of the same compound. A compound with a surface diffusivity of 10^{-12} m^2/s at 298 K would have a surface diffusivity of 10^{-29} m^2/s at 77 K, according to Rhead,[42,43] who found the following equation to

Table I. Predictions of Different Stress-Corrosion Cracking Models*

Procedure Number	Slip Dissolution	Surface Mobility	Adsorption	Film-Induced Cleavage	Actual Result
1: At 1.05 V	C iff $i_{ct} \approx$ 6,000 A/cm^2	C iff $D_s \approx 10^{-12}$ m^2/s	C	C	C
2: Aged layer	N/A	N/A	N/A	NC	NC
3: With layer, 77 K	NC	NC	NC	C	C
4: With layer, 77 K, then aged	NC	NC	NC	NC	NC
5: No layer, 298 K	NC	NC	NC	NC	NC
6: No layer, 77 K	NC	NC	NC	NC	NC

*C = cracking; NC = no cracking; and N/A = not applicable.

correlate the effect of temperature on surface diffusivity for many compounds:

$$D_s(\mathrm{m^2 s^{-1}}) = 1.4 \times 10^{-7} \exp(-13T_m/RT)$$
$$\text{if } T \ll T_m$$

Such a surface diffusivity at 77 K would predict a crack velocity of 5×10^{-15} m/s. The results of procedure 3 indicate a crack velocity very similar to that obtained by using procedure 1 (5×10^{-3} m/s). Thus, the surface diffusivity model is also inconsistent with the experimental results.

The adsorption-induced plasticity model of Lynch[7] and the stress-sorption model of Uhlig[9] are not readily quantifiable. However, they would not correctly predict the results of procedure 3. At 77 K, the possibility of migration along the growing crack of any aggressive species from the frozen environment is remote and certainly impossible at a rate sufficient to account for the observed crack velocities. Hence, adsorption models can also be ruled out as explanations for the observed cracking.

On the basis of these arguments, it can be concluded that the film-induced cleavage model is the only proposed model consistent with all of the experimental results. The formation of a nanoporous gold surface layer allows a crack to reach a velocity sufficient to allow it to propagate into the bulk (uncorroded) material. It is interesting to note that, as in the case of α-brass in ammonia,[25] both IG and TG cracks occur. However, in the latter case, the TG cracks dominate, whereas under the present experimental conditions, IG cracks are responsible for failure of the specimen.

As mentioned above, both IG and TG cracks are observed to propagate through the dealloyed layer into the bulk material (Figure 3). This is identical to the results obtained for α-brass/ammonia,[25] where both types of brittle cracking were observed, and lends further support to the proposal made in that work that IG-SCC is normally a stepwise brittle process in systems that show TG-SCC. In the α-brass in ammonia system,[25] TG cracks dominated the fracture, with IG cracks being much less prevalent under the particular test conditions used. In the present work, the IG cracks were responsible for the fracture of the specimen, and the TG cracks were less prevalent. Varying the thickness of the dealloyed layer also changed the prevalence and length of the IG and TG cracks, as will be reported in more detail elsewhere.[40]

The results of procedures 2 and 4 have shown that allowing the dealloyed layer to age destroys its ability to nucleate a crack that propagates into the bulk material. In previous work,[10,11,25] similar observations have been interpreted in terms of the coarsening of the nanoporosity of the dealloyed layer. There is substantial evidence that such coarsening occurs under conditions similar to those reported here in related work[44,49] as well as in the literature.[45–48] Pickering studied a very similar situation in his investigation of the surface roughening during the dealloying of Cu-Au alloys in 1 M H_2SO_4.[45] As part of that work, the interfacial capacitance (which is directly proportional to the surface area under the test conditions used) was followed both during the dealloying as well as after the removal of the applied current during the initial aging of the layer. In the first two minutes after the applied dealloying current was turned off, the capacitance (and, by inference, the surface area) decreased by 40 pct. This was postulated to have occurred *via* surface diffusion, in accord with the results of Wagner,[46] Gerischer and Tischer,[47] and Jaenicke and Schilling[48] for other metallic surfaces under comparable conditions. While the atomistics of the process are not clear at this time, this coarsening somehow affects the mechanical properties of the dealloyed layer and its relation to the substrate. Li[49] has shown that the coarsening of completely dealloyed three-point bend specimens of an Ag/Au alloy leads to a brittle-to-ductile transition as the pore size increases. Thus, as the coarsening increases the ligament width past a critical size, the layer loses its ability to sustain crack velocities high enough to inject the crack into the substrate. This phenomenon should not be confused with the macroscopically brittle nature of coarse, porous layers as studied by Cassagne *et al.*,[33] in which the layers were microscopically ductile (*i.e.*, the individual ligaments fail in a ductile manner). In the layers which failed in a brittle manner in the present work, fracture occurred without necking or other conventional ductile failure modes in individual ligaments.

The work reported in this paper and elsewhere[40] confirms that dealloying is able to nucleate brittle fracture in fcc alloys. Since dealloying has been shown to correlate with SCC in austenitic stainless steels,[50] it is possible that they fail by the same mechanism. In other systems showing TG-SCC (*e.g.*, steel in anhydrous ammonia, $CO/H_2O/CO_2$, or oxygenated high-temperature water[51,52,53]), other special surface layers have been proposed (nitrides,[54] carbides,[55] and ingrowing oxides (Fe_3O_4),[56] respectively). The TG cracking of pure copper[57] remains unexplained, as the original suggestion of cleavage nucleated by a Cu_2O film[58] appears dubious.[59]

The methodology used in the present investigation may appear irrelevant to the normal conditions under which SCC is known to occur. Tests on thin foils at high strain rates in liquid nitrogen may seem to have little to do with the SCC of bulk material at low strain rates at room temperature and above. The importance of the high strain rates is to effectively decouple the effects of stress and corrosion in the SCC process. As discussed above, only two types of models predict that such a decoupled system can still allow cracks to propagate: HE and the film-induced cleavage. Therefore, if tests are performed in which the stress and corrosion are decoupled and no cracking occurs (easily observable in thin foils), then this would cast doubt on the applicability of these models for that system, assuming the crack tip conditions have been well simulated. If such tests do cause cracking, dissolution can be ruled out, as the crack tip current density would be too high to be physically realizable in a real crack due to limitations by ohmic and diffusional effects. The tests in liquid nitrogen are useful in determining the role of the liquid environment and adsorption in the cracking process, as well as being an independent test for the role of dissolution. Of course, the liquid nitrogen test is discriminating only for fcc materials. Tests for aging effects are also useful in determining if the cracks had formed during the "corrosion-only" portion of the test due to residual stresses. In most cases, as mentioned, it would be difficult to separate hydrogen effects

from film-induced cleavage. However, in two systems—the present case of Au/Ag and α-brass in ammonia[25]—hydrogen evolution is impossible or highly unlikely, respectively. In summary, while these thin foil tests are not designed to replace slow strain rate testing as a means of screening alloys for service, they do provide a methodology for determining the applicability of different SCC models.

V. CONCLUSIONS

1. The brittle nature of SCC of Ag/Au has been unambiguously demonstrated.
2. This work lends strong support to the applicability of the film-induced cleavage model of SCC to IG cracking as well as TG cracking.
3. To our knowledge, this work represents the first demonstration of brittle IG-SCC (as opposed to IG-HE). Transgranular cracks that had propagated well into the bulk material after initiation in the dealloyed layer were also observed.
4. In accordance with the predictions of the film-induced cleavage model, aging of the dealloyed material reverses the embrittlement. This is most likely due to the coarsening of the nanoporous gold layer.

ACKNOWLEDGMENTS

One of the authors (RGK) acknowledges the financial support of the Fulbright Commission and the National Science Foundation through a Fulbright Scholarship and an NSF/NATO Postdoctoral Fellowship, respectively. The Research Corporation Trust is acknowledged for additional financial support, as is Johnson Matthey, plc for the loan of the materials.

REFERENCES

1. F.P. Ford: in *Embrittlement by the Localized Crack Environment*, R.P. Gangloff, ed., TMS-AIME, Warrendale, PA, 1984, pp. 117-47.
2. F.A. Champion and H.L. Logan: *J. Res. Nat. Bur. Stand.*, 1952, vol. 48, pp. 99-105.
3. D.A. Vermilyea: *J. Electrochem. Soc.*, 1972, vol. 119, pp. 405-07.
4. R.A. Oriani: in *Stress Corrosion Cracking and Hydrogen Embrittlement of Iron Base Alloys*, NACE, Houston, TX, 1973, pp. 351-58.
5. H.K. Birnbaum: in *Atomistics of Fracture*, R.M. Latanision and J.R. Pickens, eds., Plenum Press, New York, NY, 1983.
6. H. Vehoff and W. Rothe: *Acta Metall.*, 1983, vol. 31, pp. 1781-93.
7. S.P. Lynch: *Acta Metall.*, 1988, vol. 36, pp. 2639-61.
8. N.J. Petch and P. Stables: *Nature* (London), 1952, vol. 169, pp. 842-43.
9. H.H. Uhlig: in *Fundamental Aspects of Stress Corrosion Cracking*, R.W. Staehle, A.J. Forty, and D. van Rooyen, eds., NACE, Houston, TX, 1969, p. 86.
10. K. Sieradzki and R.C. Newman: *Phil. Mag. A*, 1985, vol. 51, pp. 95-132.
11. K. Sieradzki and R.C. Newman: *J. Phys. Chem. Solids*, 1987, vol. 48, pp. 1101-13.
12. C. Edeleanu and A.J. Forty: *Phil. Mag.*, 1960, vol. 46, p. 521.
13. J.R. Galvele: *Corros. Sci.*, 1987, vol. 27, pp. 1-33.
14. F.P. Ford: in *Corrosion Processes*, R.N. Parkins, ed., Applied Science Publishers, Barking, Essex, United Kingdom, 1982.
15. R.N. Parkins: *Corros. Sci.*, 1980, vol. 20, pp. 147-66.
16. A. Rota and H. Böhni: in *Electrochemical Methods in Corrosion Research*, B. Elsener, ed., Trans Tech Publications Ltd., Zurich, Switzerland, 1989, p. 177.
17. L. Graf and J. Budke: *Z. Metallkd.*, 1955, vol. 46, p. 378.
18. L. Graf: in *Fundamental Aspects of Stress Corrosion Cracking*, R.W. Staehle, A.J. Forty, and D. van Rooyen, eds., NACE, Houston, TX, 1969, pp. 187-201.
19. R.C. Newman, K. Sieradzki, and H.S. Isaacs: *Metall. Trans. A*, 1982, vol. 13A, pp. 2015-26.
20. E.N. Pugh: *Corrosion*, 1985, vol. 41, pp. 517-46.
21. A.K. Tiller: in *Stress Corrosion Cracking and Hydrogen Embrittlement of Iron Base Alloys*, NACE, Houston, TX, 1973, pp. 332-50.
22. A. Turnbull: in *Embrittlement by the Localized Crack Environment*, R.P. Gangloff, ed., TMS-AIME, Warrendale, PA, 1984. pp. 3-31.
23. U. Bertocci: *J. Electrochem. Soc.*, 1989, vol. 136, pp. 1887-92.
24. C.D. Beachem: *Metall. Trans.*, 1972, vol. 3, pp. 437-51.
25. R.C. Newman, T. Shahrabi, and K. Sieradzki: *Scripta Metall.*, 1989, vol. 23, pp. 71-74.
26. R.N. Parkins: in *Environment Sensitive Fracture: Evaluation and Comparison of Test Methods*, S.W. Dean, E.N. Pugh, and G.M. Ugiansky, eds., ASTM, Philadelphia, PA, 1984, p. 5.
27. K. Sieradzki and R. Li: Johns Hopkins University, Baltimore, MD, unpublished research, 1988.
28. P.M. Ajayan and L.D. Marks: *Phys. Rev. Lett.*, 1988, vol. 60, pp. 585-87.
29. E.N. Pugh, J.V. Craig, and A.J. Sedriks: in *Fundamental Aspects of Stress Corrosion Cracking*, R.W. Staehle, A.J. Forty, and D. van Rooyen, eds., NACE, Houston, TX, 1969, p. 118.
30. R. Bakish and W.D. Robertson: *Trans. AIME*, 1956, vol. 206, pp. 1277-82.
31. R. Bakish and W.D. Robertson: *Acta Metall.*, 1956, vol. 4, pp. 342-51.
32. T.B. Cassagne, W.F. Flanagan, and B.D. Lichter: *Metall. Trans. A*, 1988, vol. 19A, pp. 281-92.
33. T.B. Cassagne, W.F. Flanagan, and B.D. Lichter: *Metall. Trans. A*, 1986, vol. 17A, pp. 703-10.
34. B.D. Lichter, T.B. Cassagne, W.F. Flanagan, and E.N. Pugh: *J. Microstruct. Sci.*, 1985, vol. 13, pp. 361-78.
35. G.S. Duffo and J.R. Galvele: *Corros. Sci.*, 1988, vol. 28, pp. 207-10.
36. A.J. Forty and P. Durkin: *Phil. Mag. A*, 1980, vol. 42, pp. 295-318.
37. K. Sieradzki, R.R. Corderman, K. Shukla, and R.C. Newman: *Phil. Mag. A*, 1989, vol. 59, p. 713.
38. H.W. Pickering and P.R. Swann: *Corrosion*, 1963, vol. 19, pp. 373t-89t.
39. K. Sieradzki, J.S. Kim, A.T. Cole, and R.C. Newman: *J. Electrochem. Soc.*, 1987, vol. 134, pp. 1635-39.
40. R.G. Kelly and R.C. Newman: UMIST, Manchester, United Kingdom, unpublished research, 1989.
41. J.R. Rice and M.A. Johnson: in *Inelastic Behavior of Solids*, M.F. Kanninen, W.F. Adler, A.R. Rosenfield, and R.J. Jaffee, eds., McGraw-Hill, New York, NY, 1970, p. 641.
42. G.E. Rhead: *Surf. Sci.*, 1969, vol. 15, pp. 353-57.
43. G.E. Rhead: *Surf. Sci.*, 1970, vol. 22, pp. 223-28.
44. A.J. Young, R.G. Kelly, and R.C. Newman: *1st Int. Symp. on Electrochemical Impedance Spectroscopy*, Bombannes, France, May 1989.
45. H.W. Pickering: *J. Electrochem. Soc.*, 1968, vol. 115, pp. 690-94.
46. C. Wagner: *J. Electrochem. Soc.*, 1950, vol. 97, p. 71.
47. H. Gerischer and R.P. Tischer: *Z. Electrochem.*, 1954, vol. 58, p. 819.
48. W. Jaenicke and B. Schilling: *Z. Electrochem.*, 1962, vol. 66, p. 563.
49. R. Li: Ph.D. Dissertation, Queens College, City University of New York, Queens, NY, 1989.
50. R.C. Newman, R.R. Corderman, and K. Sieradzki: *Br. Corros. J.*, 1989, vol. 24, pp. 143-48.
51. B.E. Wilde: *Corrosion*, 1981, vol. 37, pp. 131-41.

52. A. Brown, J.T. Harrison, and R. Wilkins: in *Stress Corrosion Cracking and Hydrogen Embrittlement of Iron Base Alloys*, NACE, Houston, TX, 1973, pp. 686-95.
53. J. Congleton, T. Shoji, and R.N. Parkins: *Corros. Sci.*, 1985, vol. 25, pp. 633-50.
54. R.C. Newman, W. Zheng, C.R. Tilley, and R.P.M. Procter: Paper 568, *Corrosion '89*, NACE, Houston, TX, 1989.
55. I.M. Hannah, R.P.M. Procter, and R.C. Newman: in *Hydrogen Effects on Material Behavior*, N.R. Moody and A.W. Thompson, eds., TMS-AIME, Warrendale, PA, 1990, pp. 965-73.
56. R.C. Newman and K. Sieradzki: in *Chemistry and Physics of Fracture*, R.M. Latanision and R.H. Jones, eds., Martinus Nijhoff Publishers, Dordecht, The Netherlands, 1987, pp. 597-611.
57. E. Meletis and R.F. Hochman: *Corros. Sci.*, 1984, vol. 26, pp. 63-90.
58. K. Sieradzki, R.L. Sabatini, and R.C. Newman: *Metall. Trans. A*, 1984, vol. 15A, p. 1941-46.
59. U. Bertocci, E.N. Pugh, and R.E. Ricker: in *Environment Induced Cracking of Metals*, R.P. Gangloff and M.B. Ives, eds., NACE, Houston, TX, 1990, pp. 273-85.